DESIGN OF C-BAND STANDING-WAVE ACCELERATING STRUCTURE*

S. H. Kim#, B. Park, H. R. Yang, S. D. Jang, Y. G. Son,
S. J. Park, J. S. Oh, M.H. Cho and W. Namkung
POSTECH, Pohang 790-784, Korea

Abstract

We design a C-band standing-wave accelerating structure for a compact electron linac. It is capable to produce electron beams with the beam energy of 4 MeV and the pulsed beam current of 50 mA. It is to be operated in the π/2 mode with the on-axis coupled structure. The beamline is composed of the E-gun and the accelerating column with 3 and half bunching cells and 9 and half normal cells. We design standing-wave RF cavities using the OMEGA3P code to implement the asymmetric magnetic coupling slots. For the beam dynamics study, we use the PARMELA code with the SUPERFISH fields configuration. Without the pre-buncher cavity and the focusing magnets, the lost beam power to the wall is 10 kW for the output beam power of 200 kW, while the transmission is 58%.

INTRODUCTION

The electron accelerator is widely used for industrial applications, for example, contraband detection, material processing, medical diagnosis and therapy, food sterilization, and environmental processing [1]. The environmental processing such as DeSOx or DeNOx and the sterilization processing requires the average beam power of several tens of kilowatts which depends on the processing speed. The contraband detection requires 5-10 MeV with the pulsed beam current of about 150 mA [2, 3].

We are developing an electron accelerator for an X-ray source. It uses a C-band 5-GHz RF source developed for the low-power tests on the LHCD system of KSTAR. With 1.5-MW input RF power, we designed an accelerating structure capable of producing 4 MeV at the 50-mA pulsed beam current. For compactness, a standing-wave bi-periodic structure is adopted with the π/2 mode. In this paper, we present design details of the RF cavity and the beamline with the beam dynamics.

ACCELERATOR SYSTEM

The accelerator uses a 5-GHz CPI magnetron as an RF source. It is capable of producing 1.5-MW RF with the 4-μs pulse length and the 200-Hz repetition rate. The WR187 waveguide network transports the RF power to the accelerating column. This waveguide is worked under atmospheric pressure SF6 gas except the pump-out-port waveguide which is connected to the input coupler of the accelerating column. The pulse modulator supplies the 40-kV and 90-A pulsed power to the magnetron with the 4-μs pulse length [4]. It also supplies the 40-kV pulsed voltage to the E-gun. The E-gun is a diode-type thermionic DC gun.

The accelerating column is attached to the E-gun directly as shown in Figure 1. For the compact structure, a pre-buncher cavity with a drift tube is omitted. Furthermore, any solenoids magnet is not used since the beam current is low enough to be focused by the intrinsic focusing effect of the standing-wave electric field [5].

Table 1: Accelerator Parameters.

Accelerator Parameters	
Operating Frequency	5 GHz
Input RF Power (pulsed)	1.5 MW
Pulse Length	4 μs
Repetition Rate	200 Hz
E-gun Voltage	40 kV
Output Beam Energy	4 MeV
Output Beam Current (pulsed)	50 mA
Beam Transmission Rate	58%
Output Beam Power (pulsed)	200 kW
Loss Beam Power (pulsed)	10 kW
Type of Structure	Bi-periodic, On-axis coupled
Operating Mode	SW π/2 mode
Aperture Diameter	10 mm
Average Accelerating Gradients	10.7 MV/m
Number of Cells	13
Inter-cell Coupling	6.2%
Quality Factor*	7500
Effective Shunt Impedance*	90 MΩ/m
Transit-time Factor*	0.81

*Values for normal cells.

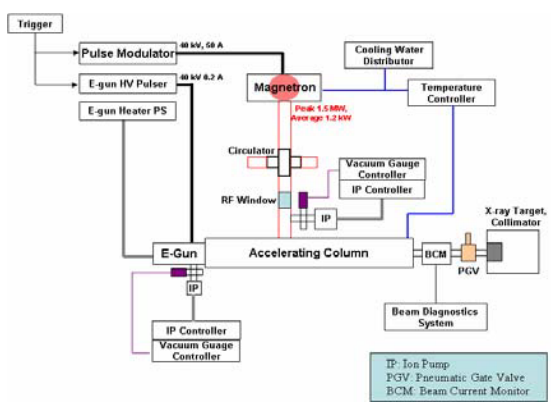

Figure 1: Block diagram of accelerator system.

*Work supported by PAL.
#khan777@postech.ac.kr

For the accelerating structure, a bi-periodic and on-axis coupled structure is adopted. Since the electric inter-cell coupling is too low due to the nose-cone, the magnetic coupling slot is bored on the wall between the accelerating cavity and the coupling cavity. The detailed design of the cavity is described in the next section and the accelerating structure in the BEAM DYNAMICS section.

CAVITY DESIGN

A bi-periodic accelerating structure has the following dispersion relation [6].

$$k_{AC}^2 \cos^2\varphi = [1-(\omega_A^2/\omega^2)+k_{AA}\cos 2\varphi] \times[1-(\omega_C^2/\omega^2)+k_{CC}\cos 2\varphi], \quad (1)$$

where ω is the resonance frequency of the coupled cavities at the φ mode, ω_A and ω_C are the resonance frequency of the accelerating cavity and the coupling cavity, and k_{AC} is the coupling coefficient between the accelerating cavity to the nearest coupling cavity, while k_{AA} for two neighbouring accelerating cavities and k_{CC} for two neighbouring coupling cavities. The design goal is to eliminate the stop band ($\omega_A - \omega_C$) and make k_{AA} and k_{CC} to be nearly zero. Also the resonance frequency at the π/2 mode should be the working frequency, 5 GHz [7].

The shape and significant dimensions of the normal accelerating cell is shown in Figure 2. The aperture diameter is 10.00 mm and the wall thickness is 3.00 mm. The gap distance between nose-cones is 16.67 mm. This model is simulated by the OMEGA3P code [8], a 3-D eigen-mode solver. The simulation is conducted for a normal cell, consisted of a coupling cavity and 2-half accelerating cavities, to find 0-, π/2-, and π-mode frequencies of the accelerating cavity. To find the π/2-mode frequency of the coupling cavity, the simulation is also conducted for a normal cell consisted of an accelerating cavity and 2 half coupling cavities.

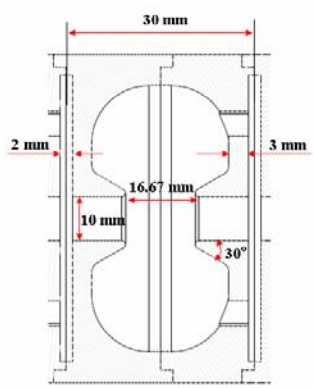

Figure 2: Crosssectional view of normal accelerating cell with significant dimensions.

With 290,000 mesh cells, the resonant frequency is 4999.88 MHz and the stop band is less than 0.5 MHz. The magnetic coupling slot on the wall is for the purpose of increasing the inter-cell coupling, since the electric coupling is not enough due to the nose-cone. Since the resonance frequency at the 0 mode is 5143.36 MHz and the frequency at the π mode is 4833.86 MHz, the k_{AA} and k_{CC} is nearly zero. The reason why the 0 mode frequency is larger than the π mode is due to the magnetic coupling slot [9]. With this mode separation, the inter-cell coupling coefficient is 6.2%.

BEAM DYNAMICS

For the beam dynamics study, the SUPERFISH and PARMELA codes are used. We assume that asymmetric fields due to the magnetic coupling slot do not affect the beam dynamics result significantly. Without any solenoid magnet and pre-buncher cavity, the beamline is composed of the E-gun and the accelerating structure with the bunching section as shown in Figure 3.

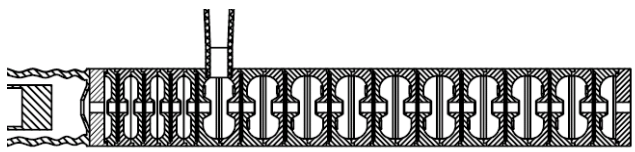

Figure 3: Accelerator column crosssectional view, position of the magnetic coupling slots are skewed to the plane of this crosssection.

The normal section is consisted of 9 and half identical normal cells with the phase velocity of c. The bunching section has 3 and half bunching cells with the phase velocity of 0.6c. For simple fabrications and measurements, the bunching cells are the same. When the phase velocity of bunching cell is 0.5c, there are significant loss at the position between the bunching section and the normal section. On the other hand, if the phase velocity is 0.7c, most of electrons can not be captured to the bunching section. The number of bunching cells is determined according to the result in Table 2, which shows that the second condition is for the optimum beam energy and transmission ratio with the acceptable beam loss power.

Table 2: Beam characteristics with number of bunching cells. The phase velocity of bunching cells is 0.6c.

	Loss Beam Power / Output Beam Power	Transmission Ratio	Beam Energy
2 & half	4.7%	50%	2.5 MeV
3 & half	4.9%	58%	4.0 MeV
4 & half	17.1%	53%	3.6 MeV

The beam dynamics simulation is conducted in consideration of the beam-loading effect. The average axial electric field is defined by

$$E_0 L = \sqrt{r_s P} - i_b r_s , \quad (2)$$

where r_s is the shunt impedance, P is the input RF power, i_b is the electron beam current, and L is the cavity length. Since the voltage, the electric field times the cavity length, is proportional to the shunt impedance of each cavity, the electric fields in the whole accelerating column is distributed as shown in Figure 4.

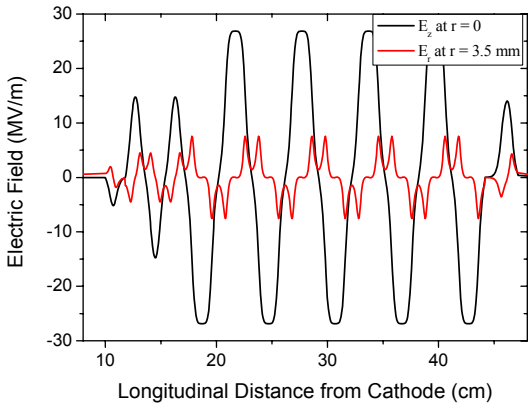

Figure 4: Electric fields in the accelerating column.

Since there is no focusing magnet, the electron beams are focused by the RF focusing effect induced by the standing-wave electric fields. In the low-energy region of Figure 5, including the bunching section, the RMS beam size is oscillating. The electron beams is still lost with the aperture in the end of accelerating column. But most of beam loss occurred in the bunching section. 91% of the lost beam has the energy lower than 1 MeV.

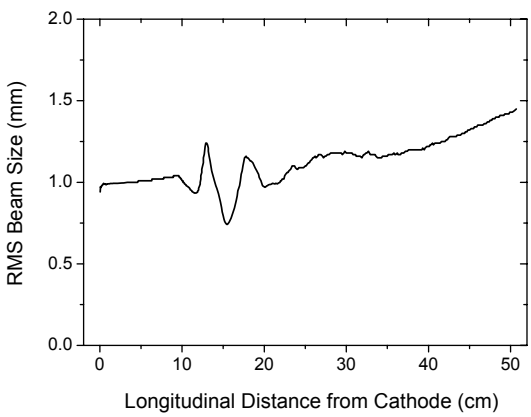

Figure 5: RMS transverse beam size, the entrance of the accelerating column is placed at 10 cm far from the cathode.

CONCLUSION

For the electron accelerator of 4 MeV and pulsed 50 mA with 1.5-MW RF source, the bi-periodic accelerating structure is designed with on-axis coupling. With the OMEGA3P code simulation, the cavity dimensions are determined for the π/2-mode frequency to be 5 GHz with 6.2% inter-cell coupling. In this geometry, the stop band is vanished. Without the pre-buncher and the solenoid magnet, this compact accelerator can make 4-MeV and 50-mA electron beams with 5% beam power loss. As the following step, cold tests for aluminium prototype of the bunching and normal cell are scheduled. Using these results, we will fabricate whole structure of the accelerating structure, braze it, and conduct fine tuning.

ACKNOWLEDGEMENT

This work is supported by PAL. The authors appreciate Dr. Luo Yingxiong at IHEP, Beijing for his advice on the accelerator system and the cavity design.

REFERENCES

[1] A. M. M. Todd, "Emerging Industrial Applications of Linacs," in *Proc. of Intl. LINAC Conf.* (Chicago, IL, August 23-28, 1998), 1036 (1998).

[2] V. Pirozhenko, et al. "Complex for X-ray Inspection of Large Containers," in *Proc. of EPAC 2006* (Edinburgh, Scotland, June 26-30, 2006), 2388 (2006).

[3] C. Hao, et al, "A New Type SW Linac Used in Industrial CT," in *Proc. of APAC 2004* (Gyeongju, Korea, March 22-26, 2004), 429 (2004).

[4] S. D. Jang, Y. G. Son, J. S. Oh, Y. S. Bae, H. G. Lee, S. I. Moon, M. H. Cho and W. Namkung, J. Korean Phys. Soc. **49**, 309 (2006).

[5] L. Auditore, R. C. Barna, De Pasquale, A. Italiano, A. Trifiro, and M. Trimarchi, Phys. Rev. ST-AB **7**, 030101 (2004).

[6] E. A. Knapp, B. C. Knapp, and J. M. Potter, Rev. Sci. Instr. **39**, 979 (1968).

[7] H. Euteneuer, A. Jankowiak, M. Negrazus, and V. I. Shvedunov, "The 4.9 GHz Accelerating Structure for MAMI C," in *Proc. of EPAC 2000* (Vienna, Austria, June 26-30, 2006), 1954 (2006).

[8] ANALYST with the OMEGA3P code is a trademark of STAR, inc.

[9] T. Shintake, "Analysis of the transient response in periodic structures based on a coupled-resonance model," in *Proc. of Joint US-CERN-Japan International School* (Hayama/Tsukuba, Japan, Sep. 9-18, 1996), 335 (1999).